*Adaptive* **Behavior**

# Synchrony and phase relation dynamics underlying sensorimotor coordination

**Bruno A Santos[1,2], Xabier E Barandiaran[3] and Philip Husbands[1]**

## Abstract

Synchronous oscillations have become a widespread hypothetical "mechanism" to explain how brain dynamics give rise to neural functions. By focusing on synchrony one leaves the phase relations during moments of desynchronous oscillations either without a clear functional role or with a secondary role such as a transition between functionally "relevant" synchronized states. In this work, rather than studying synchrony we focus on desynchronous oscillations and investigate their functional roles in the context of a sensorimotor coordination task. In particular, we address the questions: a) how does the informational content of the sensorimotor activity present in a complete dynamical description of phase relations change as such a description is reduced to the dynamics of synchronous oscillations? and b) to what extent are desynchronous oscillations as causally relevant as synchronous ones to the generation of functional sensorimotor coordination? These questions are addressed with a model of a simulated agent performing a functional sensorimotor coordination task controlled by an oscillatory network. The results suggest that: i) desynchronized phase relations carry as much information about sensorimotor activity as synchronized phase relations; and ii) phase relations between oscillators with near-zero frequency difference carry a relatively higher causal relevance than the rest of the phase relations to the sensorimotor coordination; however, overall a privileged functional causal contribution can not be attributed to either synchronous or desynchronous oscillations.

## 1 Introduction

*Synchrony* has become the hypothetical "mechanism" that is repeatedly invoked to explain how spatially segregated neural oscillators get integrated into functional transient clusters giving rise to cognitive functions such as coherent sensorimotor coordination, perception and conscious experience (Engel, Konig, Gray & Singer, 1990; Fries, 2005; Gray & Singer, 1989; Hipp, Engel & Siegel, 2011; Pockett, Bold & Freeman, 2009; Singer, 2011; Tononi & Edelman, 1998; Uhlhaas et al., 2009; Varela, Lachaux, Rodriguez, & Martinerie, 2001; von der Malsburg, 1981). Synchrony refers only to one aspect of the temporal relation among oscillatory signals: i.e. that in which the phase relation between oscillatory signals remains (relatively) constant. A dynamical description of an oscillatory network in terms of its synchronous transient clusters is a reduced description from its entire phase relation dynamics; that is, it does not take into consideration how the phase relations between desynchronized oscillators are changing over time. Such a reduction in the dynamical

description might be leaving out of the equation moments of oscillatory dynamics that are relevant for neural functions.

In this work, rather than studying synchrony we focus on desynchronous oscillations and investigate their relevance in the context of an embodied oscillatory network generating a functional sensorimotor coordination. The first problem we address is the following: *how does the informational content of the sensorimotor coordination present in a complete dynamical description*

[1]Centre for Computational Neuroscience and Robotics, University of Sussex, UK
[2]Laboratory of Intelligent Systems, CEFET-MG, Belo Horizonte, Brazil
[3]Department of Logica and Philosophy of Science, University of the Basque Country, Spain

**Corresponding author:**
Bruno Santos, Centre for Computational Neuroscience and Robotics, John Maynard Smith Building, University of Sussex, Falmer, Brighton, BN1 9QG, UK
Email: b.santos@sussex.ac.uk

*of phase relations change as such a description is reduced to the phase relations of synchronous oscillations?* That is, it is studied how the amount of information available about the sensorimotor coordination changes as the phase relations of desynchronous oscillations are left out of the dynamical description of the oscillatory network. Though it is expected that the amount of information in a reduced description is smaller than or equal to the information in a more complete one, it is relevant to analyze *how* this amount of information changes. By doing this analysis it is possible to identify whether there are ranges of phase relations – during synchronized activity, for instance – that carry more information than others about the sensorimotor dynamics.

The second problem we address is the following: *to what extent are desynchronous oscillations as causally relevant as synchronous oscillations to the generation of functional sensorimotor coordination?* The causal relevance is quantified by the effects on the sensorimotor coordination of an agent after applying perturbations to the oscillatory network during moments of synchronization or desynchronization. This study identifies whether there are ranges of phase relations – during synchronous oscillations, for instance – that carry a higher functional causal contribution to the generation of coherent sensorimotor coordination.

The analyzes of informational content (first problem) and causal relevance (second problem) of the phase relations during synchronous and desynchronous oscillations contribute to the understanding of oscillatory dynamics underlying sensor and motor activities; it might also provide insight into works that attribute a privileged explanatory status to synchronous oscillations over desynchronous ones. Both problems are addressed using a model of a simulated agent performing phototatic behavior and controlled by a network of phase-coupled oscillators.

This paper is organized as follows. In the next section some works that focus on synchronous oscillations are briefly presented. Then the concepts of a complete and a reduced dynamical descriptions of an oscillatory network are formalized. This formalization will make clearer the problem and methods approached in this work. Following up, the mathematical model of the embodied oscillatory network, analyses, results and conclusions are presented.

## 2 Background

The first scientist to observe and describe synchrony in oscillatory systems was probably Huygens (1973) who studied the mutual synchronization of pendulum clocks coupled by a beam (Pikovsky, Rosenblum & Kurths, 2003). Since then, synchrony has been studied in different phenomena in the natural world, in physics and engineering. Some examples are: circadian oscillators which are used by biologists to explain mechanisms underlying behavioral modifications (Gardner, Hubbard, Hotta, Dodd & Webb, 2006); glycolytic oscillations in yeast cells (Dano, Sorensen & Hynne, 1999), chirp synchronization in crickets (Walker, 1969), and synchronization in arrays of lasers (Kozyreff, Vladimirov & Mandel, 2000).

The root of the approach that privileges synchrony as being functionally relevant to neural functions dates back to von der Malsbung (1981). von der Malsburg pointed out a deficiency in existing brain theory – how integration occurs among functionally distinct brain areas – and discussed at a conceptual level how to fill this gap. He proposed that fast synaptic modulation is the mechanism through which functionally different active cells become integrated and express the whole set of different features of an external object; the integrated cells are defined by their synchrony activity in a temporal fine structure of [2,5] ms resolution.

The first evidence supporting von der Malsburg's hypothesis came from empirical studies of integration in the visual cortex, a research field denoted as *the visual binding problem* (Eckhorn et al., 1988; Engel et al., 1990; Gray & Singer, 1989; Roskies, 1999). This problem can be stated as follows: *"how are the different attributes of an object brought together in a unified representation given that its various features (edges, color, motion, texture, depth and so on) are treated separately in specific visual areas?"* (Varela et al., 2001, p. 231). At a high spatial resolution, synchronized oscillations were observed among primary, secondary and associative areas of the visual cortex (Eckhorn et al., 1988) and also among visual cortex areas in both cerebral hemispheres (Engel, Konig, Kreiter & Singer, 1991).

At a larger scale, neural synchrony has also been found and hypothesized as the binding mechanism of neuronal groups spatially distributed in the cortex – not only the visual one – of animals (Bressler, Coppola & Nakamura, 1993; Roelfsema, Engel, Konig & Singer, 1997) and humans (Rodriguez et al., 1999) performing a motor behavior according to the perception of sensory stimuli. Hipp et al. (2011) provided further evidence supporting the existence of dynamic functional large-scale synchronized clusters underlying cross-modal perception in human beings. Particularly, they showed the presence of transiently synchronized clusters at beta and gamma frequencies across distributed brain areas and also found that the magnitude of synchronization in the beta and gamma networks could predict the subject's perception (visual stimulus of bars either crossing one another or bouncing off each other presented together with an auditory stimulus of a click sound).

The aforementioned works concern the privileged status attributed to synchrony as a possible mechanism to solve the integration of functionally distinct brain areas involved in the perception of sensory stimuli.

Synchrony has been argued to play an important role as the dynamical neural signature of a subject's perception (Lutz, Lachaux, Martinerie & Varela, 2002). It has also been hypothesized to be a mechanism of large-scale integration and communication that allows the brain areas to coordinate their activity giving rise to coherent behavior and cognition (Varela et al., 2001):

> The experimental evidence consistently shows that synchronous networks emerge and disappear in waves that last 100–300 ms; these transients represent a meaningful temporal scale of brain operation. (Varela et al., 2001, p. 237)

> There is some evidence that phase synchronization is accompanied by phase scattering in other bands or between different neuron pairs. We suggest that this novel observation is crucial for the understanding of large-scale integration, which must implicate not only the establishment of dynamic links, but also their active uncoupling to give way to the next cognitive moment. (Varela et al., 2001, p. 237)

Desynchronization is then left with the role of undoing the preceding "meaningful" synchronized cluster for the emergence of the next one. Such a role is also mentioned by Rodriguez et al. (1999, p. 432): *"transition between two distinct cognitive acts (such as face perception and motor response) should be punctuated by a transient stage of undoing the preceding synchrony* [by active desynchronization] *and allowing for the emergence of a new ensemble"*.

The privileged status given to synchrony is supported by empirical evidence that has suggested its causal relevance for different neural functions at least in terms of correlations with characteristically cognitive events. It is undeniable that research into oscillatory neurodynamics has made significant progress in understanding brain operation by focusing on synchrony. In this work, however, we focus on desynchronous oscillations comparing their relevance to synchronous ones.

## 3 Complete and reduced dynamical descriptions

Consider a network of $N$ phase-coupled oscillators where the periodic phase $\theta_i$ of an oscillator $i$ is given by $\theta_i(t) = f_i(\theta_1, \theta_2, \ldots, \theta_N)$. The phase relation dynamics between two oscillators $i$ and $j$ can be analyzed by the absolute value of their phase difference, as shown in equation (1)

$$\phi_{i,j}(t) = \left| \theta_i(t) - \theta_j(t) \right| \qquad (1)$$

where $\phi_{i,j}(t) \in R : [0, 2\pi)$ radians and represents how the phase relation between $i$ and $j$ is changing over time. A complete dynamical description of an oscillatory network is given by the phase relations between all

oscillatory components, as shown in equation (2), where $P$ is a vector function containing all the dynamics of phase relations between all pairs of oscillators $i$ and $j$.

$$P(t) = \langle \phi_{1,2}(t), \phi_{1,3}(t), \ldots, \phi_{i,j}(t) \rangle \qquad (2)$$

Before presenting the reduced dynamical description of $P$, we discuss two approaches to study synchronization, namely *zero-lag synchronization* and *phase synchronization*. While in the former, oscillators are said to be synchronized only when they are phase-locked at zero (or near zero) radians, in the latter, synchronization takes place when oscillators are phase-locked at any phase. Formally, we can say that $i$ and $j$ are *zero-lag synchronized* if $\dot{\phi}_{i,j} = 0$ and $\phi_{i,j} = 0$; and *phase synchronized* if $\dot{\phi}_{i,j} = 0$ and $\phi_{i,j} = c_p$, where $c_p$ is a constant $\in [0, 2\pi)$ radians. Note that zero-lag synchrony is only a particular case of phase synchronization. An important difference between these approaches is that $\pi$-phase-locked oscillators (i.e. $\dot{\phi}_{i,j} = 0$ and $\phi_{i,j} = \pi$) are considered completely desynchronized in the zero-lag synchronization approach and completely synchronized in the phase synchronization one. Oscillators could also be considered synchronized when their frequency ratio is constant (e.g. $\Omega_i = 10$ Hz and $\Omega_j = 20$ Hz with frequency ratio $1 : 2$); which, in this case, $\dot{\phi}_{i,j}$ linearly changes over time. In our work we consider that a pair of oscillators is synchronized when their frequency ratio is $1 : 1$ and when they are phase-locked at any phase $\phi_{i,j} = c_p$, which is the most studied case of synchrony in the brain (Varela et al., 2001). For more details about synchrony see Pikovsky et al. (2003) and Strogatz (2000b, p. 96).

Given this definition of synchrony, a simple dynamical description that represents how clusters of synchronized oscillators change over time can be defined as in equation (3).

$$S_a(t) = \langle x_{1,2}(t), \ldots, x_{i,j}(t) \rangle; \; x_{i,j}(t) = \begin{cases} 1 & if \; \dot{\phi}_{i,j}(t) \leqslant t_s \\ 0 & otherwise \end{cases}$$
$$(3)$$

Where $S_a$ represents how the synchronized state between each pair of oscillators is changing over time; $x_{i,j}(t)$ is a step function which gives 1 when $i$ and $j$ are phase synchronized and 0 otherwise. Notice that the synchronized condition has been changed from $\dot{\phi}_{i,j}(t) = 0$ to $\dot{\phi}_{i,j}(t) \leqslant t_s$. The parameter $t_s$ is a threshold for $\dot{\phi}_{i,j}(t)$ up to which two oscillators are considered synchronized. This relaxation of the strict $\dot{\phi}_{i,j}(t) = 0$ condition for synchrony better represents what is generally considered synchronization between neural oscillators.

The vector function $S_a$ is a reduced dynamical description of $P$ that only informs whether a pair of oscillators is either synchronized or not. A richer description of the synchronized oscillations would contain the phase relation dynamics during moments of

synchronization; i.e. it would contain the actual phase relation $\phi$ when $\dot{\phi}_{i,j} \leqslant t_s$, as shown in equation (4).

$$S_b(t) = \langle y_{1,2}(t), \ldots, y_{i,j}(t) \rangle;$$
$$y_{i,j}(t) = \begin{cases} \phi_{i,j}(t) & \text{if } \dot{\phi}_{i,j}(t) \leqslant t_s \\ \text{shuffle} & \text{otherwise} \end{cases} \quad (4)$$

Where $S_b$ is the vector function containing the phase relation dynamics between all synchronized oscillators. If the oscillators $i$ and $j$ are synchronized then the vector function contains their phase relations – i.e. if $\dot{\phi}_{i,j}(t) \leqslant t_s$, then $y_{i,j}(t) = \phi_{i,j}(t)$. On the other hand, when the oscillators $i$ and $j$ are desynchronized during a time-window $T$, i.e. $\dot{\phi}_{i,j}(t) > t_s \forall\, t \in T$, their actual values of phase relations $\phi_{i,j}$ during $T$, i.e. $\phi_{i,j}(T)$, will be shuffled. The shuffling algorithm picks each value of phase relation in $T$ and swaps it with another one from a random position in $T$. The lack of information about the phase relation dynamics – or the reduced descriptions of phase relations – is then modeled by shuffling the actual values of phase relation $\phi_{i,j}$. By doing that, potential correlations between $\phi_{i,j}$ and any other time series are removed; this will be important for measuring how the informational content of a reduced dynamical description changes in relation to a more complete one.

Both vector functions $S_a$ and $S_b$ are particular ways to represent how the core of synchronized oscillators are changing over time. While $S_a$ is a sharp reduction from P, $S_b$ can be continuously reduced from P by decreasing the parameter $t_s$. Notice that if $t_s$ is greater or equal than the maximum value of $\dot{\phi}_{i,j}$ in a time-window $T$ then the content of $S_b$ is equal to P.

## 4 Theoretical model and methods

### 4.1 Preliminary considerations

We present an evolutionary robotic model that performs phototaxis controlled by a network of five phase-coupled Kuramoto oscillators. Evolutionary robotics (Harvey, Husbands, Cliff, Thompson & Jakobi, 1997; Harvey, Paolo, Wood & Quinn, 2005; Nolfi & Floreano, 2004) is a well established field in cognitive science where genetic algorithms are used to optimize the parameters of a complex robot controller according to a particular fitness function. It has been successfully applied in different contexts including adaptive behavior (Beer, 2003), behavioral neuroscience modeling (Izquierdo & Lockery, 2010) and cognitive neuroscience (Ruppin, 2002).

Phototaxis requires the agent to approach a light source from different starting positions and can be taken as a paradigmatic example of a minimal (yet not completely trivial) "goal-directed" sensorimotor coordination task. It was chosen for simplicity as a minimal

coordination task where the problems considered in the previous section could be addressed.

Kuramoto phase-coupled oscillators (Kuramoto, 1984) have been used to study biological phenomena of collective synchronization such as pacemaker cells in the heart, circadian pacemaker cells in the brain and flashing fireflies (Strogatz, 2000a). They have been used to explore mechanisms underlying oscillations in the human cortex (Breakspear, Heitmann & Daffertshofer, 2010) and different aspects of brain dynamics such as self-organized criticality (Kitzbichler, Smith, Christensen & Bullmore, 2009). In evolutionary robotics, they have been implemented as a controllers of agents performing categorical perception (Moioli, Vargas & Husbands, 2010) and phototaxis (Santos, Barandiaran & Husbands, 2011). Kuramoto's oscillators are based on a previous model of coupled oscillators proposed by Winfree (1967, 1980), that describes the dynamics of oscillators with different natural frequencies interacting by a function representing their sensitivity to the phase of each other.

The goal of our model is not to target any specific biological mechanism or to show the potential of oscillatory controllers for complex adaptive tasks. The goal is to use the model as an exploratory tool to address the theoretical questions described above by using an embodied oscillatory network within a continuous time-closed sensorimotor loop and without assuming any a priori functional decomposition of oscillatory components.

In our model, each oscillator of the robot's controller can be interpreted in various ways: a) as chemical oscillatory dynamics controlling unicellular motility, b) as individual oscillatory neurons, c) as the activity of neuronal groups, tissues or brain regions, and d) as the macroscopic result of the activity of interactions between such regions, like EEG recordings. It is not necessary, however, to adhere to any of these levels of interpretation, we take the oscillators to be theoretical entities at an undetermined level of abstraction. What matters to us, at this stage, is not the level of empirical accuracy of the model but its capacity to raise theoretical issues and its potential to open new insights into dynamical modeling and analysis of neural oscillatory dynamics and sensorimotor activity.

As far as the analysis of the model is concerned, we mainly use tools from Information Theory (e.g. mutual information, information transfer) and Dynamical System Theory. Information-theoretic quantities have been applied to study the information flow in "isolated" oscillatory network with controlled parameters (Ceguerra, Lizier & Zomaya, 2011), and in real and simulated brain–body environment systems (Lungarella & Sporns, 2006; Pitti, Lungarella & Kuniyoshi, 2009; Williams & Beer, 2010).

## 4.2 The agent and its network of coupled oscillators

The model consists of a two-dimensional simulated environment, an agent and a light source. The agent's movement is controlled by a network of phase-coupled oscillators which receives signals from two sensors and controls the activation of two motors. The agent has a circular body of five units diameter; two sensors $s_1$ and $s_2$ separated by $120\pm10°$ and whose output signal is given by $s_q = e^{-0.04d_q}$, where $q$ represents each sensor, and $d$ is the distance from sensor $q$ to the light source. The agent has two diametrically opposed motors $m_1$ and $m_2$ whose activation is given by equations (5) and (6), respectively.

$$m_1 = (\sin(\theta_4 - \theta_3) + 1)/2 \qquad (5)$$

$$m_2 = (\sin(\theta_5 - \theta_3) + 1)/2 \qquad (6)$$

Where $\theta_n$ is the phase of the oscillator $n$. The agent's behavior is controlled by a network of five phase-coupled oscillators (Kuramoto, 1984), defined in equation (7)

$$\dot{\theta}_i = (\omega_i + s_q w_{qi}) + \sum_{j=1}^{N} k_{ji} \sin(\theta_j - \theta_i) \qquad (7)$$

where $\theta_i$ is the phase of the $i^{th}$ oscillator which is integrated with the time-step 15 ms using the Euler method, $\omega_i$ is the oscillator's natural frequency (range for the genetic algorithm [9,18] Hz), $s_q$ is the $q^{th}$ sensory signal (out of 2), $w_{qi}$ is the sensory input strength from the sensor $q^{th}$ to the oscillator $i^{th}$ (range [1,20]), $N$ is the number of oscillators (here five), and $k_{ji}$ is the coupling factor from the $j^{th}$ to the $i^{th}$ oscillator with $k_{j,i} = 0 \,\forall\, i = j$ (range [0,20]). The sensors $s_1$ and $s_2$ are connected to the oscillators $\theta_1$ and $\theta_2$, respectively; the other oscillators do not receive sensory signals.

## 4.3 Optimization with a genetic algorithm

A total of 27 network parameters encoded in a genotype as a vector of real numbers in the range [0,1] (linearly scaled, at each trial, to their corresponding range) were evolved using the *microbial genetic algorithm* (Harvey, 2001). There is no specific reason why this algorithm was chosen; the system is relatively simple and could have been optimized with other genetic algorithms. The genetic algorithm setup is: population size (80); mutation rate (0.05); recombination (0.60); reflexive mutation; normal distribution for mutation ($\mu = 0, \sigma^2 = 0.1$); trial length (180 s); and trials for each agent (30). At the end of the $30^{th}$ trial, the worst fitness (out of 30) is used as the selective fitness of the agent. The fitness function is defined by equation (8):

$$F = \begin{cases} 1 - \frac{d_f}{d_i}; & \text{if } d_f < d_i; \\ 0; & \text{otherwise}; \end{cases} \qquad (8)$$

where $F$ is the fitness; $d_i$ and $d_f$ are the initial and final distances to the light source, respectively. The analysis of the model is done using the fittest agent found by the genetic algorithm.

It was possible to optimized the parameters of the system in order to obtain an agent doing phototaxis using three and four oscillators. However, the dynamics obtained using fewer oscillators were not adequate to analyze the relevance of desynchronized oscillations as most of the time the oscillatory network was completely synchronized. Specifically, while the agent was approaching the light, the oscillators were totally synchronized and while it was moving around the light there were some short time-windows of desynchronized oscillations.

## 4.4 Methods of analysis

Our first problem is to analyze how the information about the sensorimotor dynamics in the oscillatory network changes as the description of phase relations is reduced. The agent's sensorimotor dynamics are given by a vector function shown in equation (9).

$$SM(t) = \langle s_1(t), s_2(t), m_1(t), m_2(t) \rangle \qquad (9)$$

Where $SM$ is the sensorimotor activity, $s_1$, $s_2$, $m_1$ and $m_2$ are the agent's sensors and motors. We are interested in analyzing how the mutual information between $SM$ and $S_b$ changes as the threshold $t_s$ decreases; i.e. $I(SM, S_b)$ for different values of $t_s$. As both time series are multi-dimensional, the mutual information will be measured between pairs of components from each time series – e.g. $I(SM(s_1), P(\phi_{1,2}))$ and $I(SM(m_2), P(\phi_{3,4}))$.

The analysis is carried out by using the standard measures of *entropy* and *mutual information* from information theory, as described in equations (10) and (11), respectively (Cover & Thomas, 2005; Shannon, 1948a, 1948b).

$$H(X) = -\sum_{i=1}^{N} p(x_i)\log_b(x_i) \qquad (10)$$

Where $X$ is a set of discrete random variables and $p(x_i)$ is the probability mass function of the outcome $x_i$.

$$I(X;Y) = H(X) + H(Y) - H(X,Y) \qquad (11)$$

Where $H(X)$, $H(Y)$ are the entropies of the sets $X$ and $Y$, respectively, and $H(X,Y)$ is the joint entropy of both sets. The entropies are measured based on a time-window $T$ of 6 s length. In order to obtain more robust measures of the probability distributions, all time series are linearly interpolated from a time-step of 15 ms (Euler step integration of the simulation) to 1 ms. In this way, a time-window of 6 s length contains 6000 points. In order to defined the length of $T$ the probability distributions of all individuals and pairs of
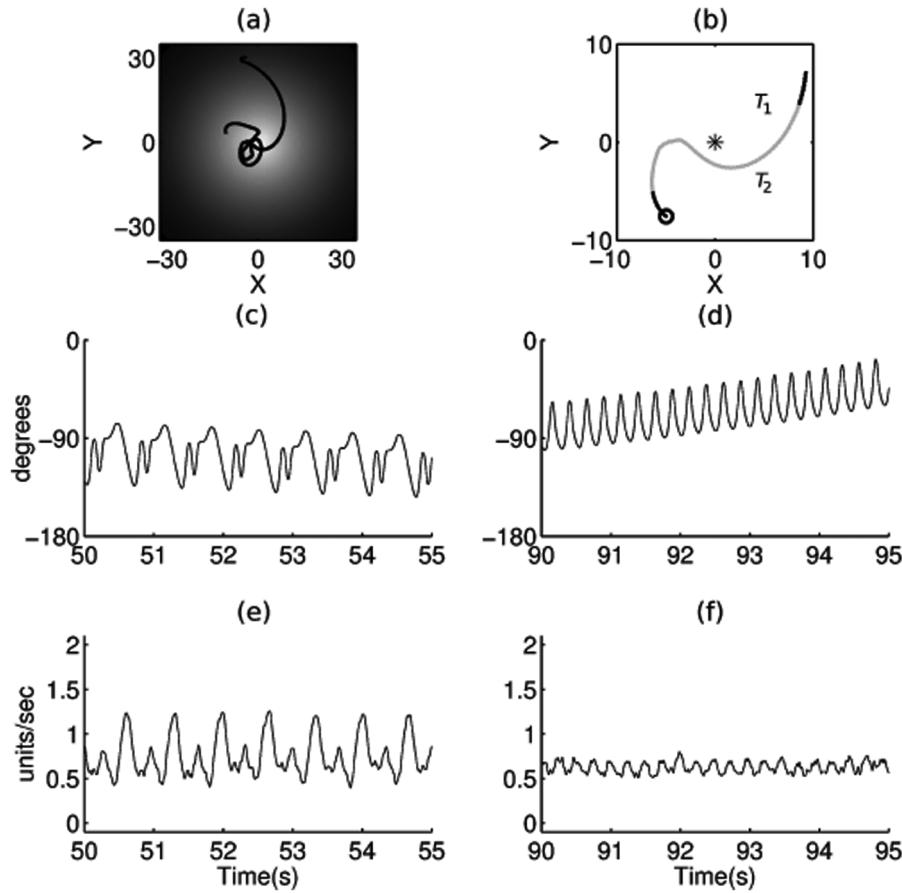
**Figure 1.** (a) shows an agent's trajectory in the environment during its lifetime (180 s). The light intensity throughout the environment is represented by the gray scale, where the whiter the area the higher the light intensity. The agent moves towards the region of highest light intensity (position $X = 0, Y = 0$) and then starts moving around it. (b) Zooms in to the agent's trajectory during $t = [50, 95]$ s;. The star at $X = 0$ and $Y = 0$ indicates the position of highest light intensity. The highlighted black trajectories indicate the agent's trajectory during two short time-windows of 5 s: $T_1 = [50, 55]$ s and $T_2 = [90, 95]$ s. (c) and (d) show the angle of the agent's body in $T_1$ and $T_2$, respectively. The agent's body continuously oscillates to the right and left following different patterns at each time-window. E) and F) show the agent's average linear speed for a moving time-window of 200 ms in $T_1$ and $T_2$, respectively. The agent's average linear speed is 0.76 units/s in $T_1$ and 0.62 units/s in $T_2$.

components – *e.g.* $H(s_1)$ and $H(m_1, \phi_{3,4})$ – were measured using different lengths from 100 ms to 7.0 s. Due to the stationarity of the time series, the distributions do not change for time-windows greater than 5.0 s. By shifting the time-window $T$ we capture how the entropies change as the agent interacts with the environment. As the values of phase relations $\phi_{i,j}$ are continuous in the interval $[0, 2\pi]$ they are discretized into 50 equally spaced bins. The sensors and motors are also discretized into 50 equally spaced bins according to their minimum and maximum value within each time-window $T$.

The second problem we are interested in studying is the causal relevance of the information transferred during the desynchronized $\dot{\phi}_{i,j} > t_s$ and synchronized $\dot{\phi}_{i,j} \lesssim t_s$ oscillations for the generation of functional sensorimotor dynamics $SM$. The causal relevance is analyzed by perturbing the information transferred in either of the conditions $\dot{\phi}_{i,j} > t_s$ or $\dot{\phi}_{i,j} \lesssim t_s$ and measuring the functionality $SM$ using the fitness function in

equation (8). More details about this problem will be presented during the presentation of the results.

## 5 Results

The results are divided into three main parts. In the first one, the dynamical analyses of $SM$, $P$, $S_a$, and $S_b$ are presented. In the second one, the analysis of mutual information between $SM$ and the reduced descriptions of phase relations $S_b$ is shown. In the third one, the causal relevance of synchronization and desynchronization for the generation of functional $SM$ is analyzed.

### 5.1 Dynamical analyses

*5.1.1 Sensorimotor dynamics (SM).* Figure 1 shows the agent's trajectory during a single trial of phototaxis. During $T_1 = [50, 55]$ s the agent's trajectory is
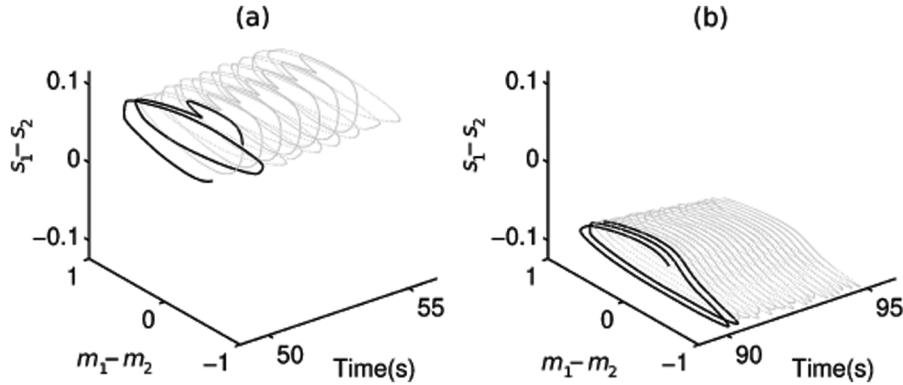
**Figure 2.** (a) and (b) show the sensorimotor dynamics $SM(t) = (s_1(t), s_2(t), m_1(t), m_2(t))$ during $T_1$ and $T_2$. The x-axis shows the time in s, the y-axis shows the difference in activation of the right and left motors ($m_r - m_l$) and z shows the difference in activation of the right and left sensors ($s_1 - s_2$). The black trajectories in both images highlight the first 600 ms of each time-window.

characterized by a movement towards the region of highest light intensity at an average linear speed of 0.76 units/s and slowly turning to the right at an average angular speed of 5.2 deg/s (not shown in the figure). In $T_2 = [90, 95]$ s the agent is returning to the region of highest light intensity at an average linear speed of 0.62 units/s and turning to the left at an average angular speed of 12.7 deg/s. The sensorimotor dynamics $SM$ for the time-windows $T_1$ and $T_2$ are presented in Figure 2 and will be referred to as $SM_{T_1}$ and $SM_{T_2}$, respectively.

In the next subsections the oscillatory dynamics underlying $SM_{T_1}$ and $SM_{T_2}$ are analyzed. These time-windows were chosen to represent two reasonably well separated periods in the overall behavior and to reflect the two main 'phases' of the behavior (approaching the light from a distance and then moving around it). There is nothing particularly special about these two periods, the main purpose is only to present dynamical descriptions of the $P$, $S_b$ and $S_a$ manifolds underlying the two moments of the agent's sensorimotor coordination during a trial of phototaxis.

### 5.1.2 Phase relation dynamics (P).
We shall start by presenting the complete phase relations of a single pair of oscillators (see Figure 3). The transient synchronization between $\theta_1$ and $\theta_5$ takes places at different phases during different periods, namely: $T_{1a} = [-48, -33]$, $T_{1c} = [33, 40]$ and $T_{2a} = [-26, 11]$ degrees, as shown in Figure 3(a) and (c) or (b) and (d).

In dynamical system terms, we can say that the attractor landscape of $\phi_{1,5}$ during $SM_{T_1}$ has low potential energy at $[-48, -33]$ and $[33, 40]$ degrees and during $SM_{T_2}$ these regions of low potential energy collapse into a single one around $[-26, 11]$ degrees. The difference in the attractor landscape is represented in graphic Figure 3(e); where positive values represent regions that have had their potential energy decreased ($[-26, 26]$) and became more attracting; negative values represent regions that have had their potential energy increased

($[-70, -26]$ and $[26, 70]$) and lost their attraction; and values near zero represent regions that did not have a significant change in their potential energy.

As $P$ has ten dimensions, we use density distributions, as shown in Figure 3(b) and (d), to show statistical properties of the components in $P$ (see Figure 4). The lower the entropy (shown on the top of the image) the longer the oscillators $i$ and $j$ (x-axis) keep synchronized at a particular phase indicated by peaks in the density distribution (the whiter areas of the image). In other words, the lower the entropy the smaller the potential energy at the phase relations represented by whiter areas.

Some differences between the phase relation dynamics underlying $SM_{T_1}$ and $SM_{T_2}$ are: while in $SM_{T_1}$, $\phi_{1,2}$ is relatively spread ($H_{(\phi_{1,2})} = 0.81$) across $\approx [0, 90]$, in $SM_{T_2}$ it has a higher phase coherence ($H_{(\phi_{1,2})} = 0.34$) within $\approx [30, 60]$; while in $SM_{T_1}$, $\phi_{2,3}$ is relatively spread ($H_{(\phi_{2,3})} = 0.82$) across $\approx [50, 140]$, in $SM_{T_2}$ it is concentrated ($H_{(\phi_{1,2})} = 0.34$) within $\approx [85, 115]$. Note that though both pairs of oscillators $(\theta_3, \theta_4)$ and $(\theta_3, \theta_5)$ that send signals to the motors have low phase coherence (indicating a low level of synchrony) – as shown by high entropies $H_{(\phi_{3,4})} = 0.97$ and $H_{(\phi_{3,5})} = 0.94$ in $SM_{T_1}$ and $H_{(\phi_{3,4})} = 0.93$ and $H_{(\phi_{3,5})} = 0.90$ in $SM_{T_2}$ – the agent's behavior is still completely functional.

### 5.1.3 Synchronization dynamics ($S_b$).
The multi-dimensional synchronization dynamics $S_b$ is also shown for the single pair of oscillators $\theta_1$ and $\theta_5$, see Figure 5. The synchronization dynamics were generated for a threshold $t_s = 15$ rad/s (see equation (3)), meaning that two oscillators are considered synchronized when their frequency difference is within $[-15, +15]$ rad/s or $[-2.39, +2.39]$ Hz. During moments of desynchronization – which can be interpreted as $\dot{\phi}_{1,5} > 15$ rad/s for this specific case – there is no information about how the phase relation is changing, shown by the shuffled phase relations in $T_{1b}$ and $T_{2b}$. The oscillators get
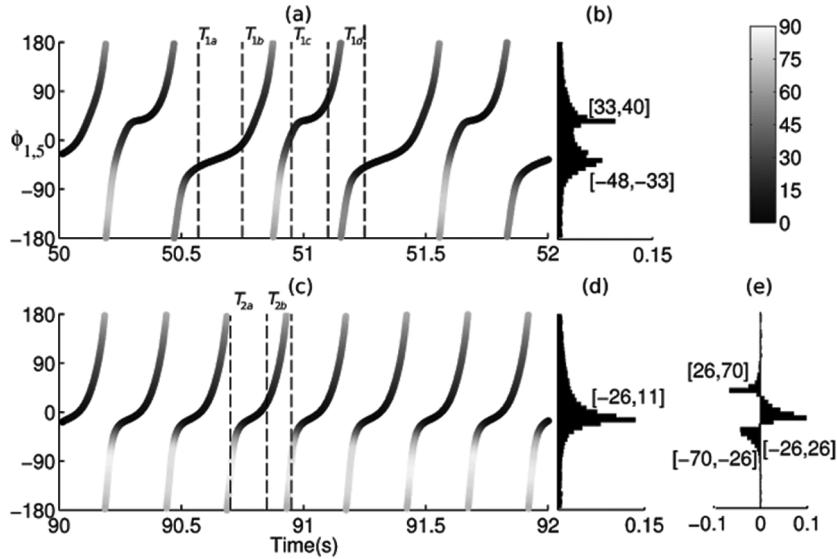
**Figure 3.** Phase relations between $\theta_1$ and $\theta_5$ ($P(\phi_{1,5})$) underlying sensorimotor regimes $SM_{T_1}$ (a) and $SM_{T_2}$ (c). The relation $\phi_{1,5}$ is shown in the y-axis and time in the x-axis. The color bar shows $\dot{\phi}_{1,5}$ in rad/s, where the darker the color the lower the derivative. For ease of description we highlight four small time-windows during $T_1$: $T_{1a}$, $T_{1b}$, $T_{1c}$ and $T_{1d}$ of 180, 200, 150 and 150 ms, respectively (see dashed lines in (a)) and other two time-windows during $T_2$: $T_{2a}$ and $T_{2b}$ of 150, 100 ms, respectively (see dashed lines in (c)). Note that the x-axis depicts only 2 s ([50,52]) rather than 5 s ([50,55]). While underlying $SM_{T_1}$ the phase relation $\phi_{1,5}$ has two regions where it slows down (see $T_{1a}$ and $T_{1c}$); underlying $SM_{T_2}$ it has only one around 0 degrees (see $T_{2a}$). This difference can be seen by the peaks of density distributions of $\phi_{1,5}$ shown in (b) and (d). These distributions were generated for the two-second time-windows [50,52] s and [90,92] s, respectively. (e) shows the difference between the density distributions shown in (b) and (d).
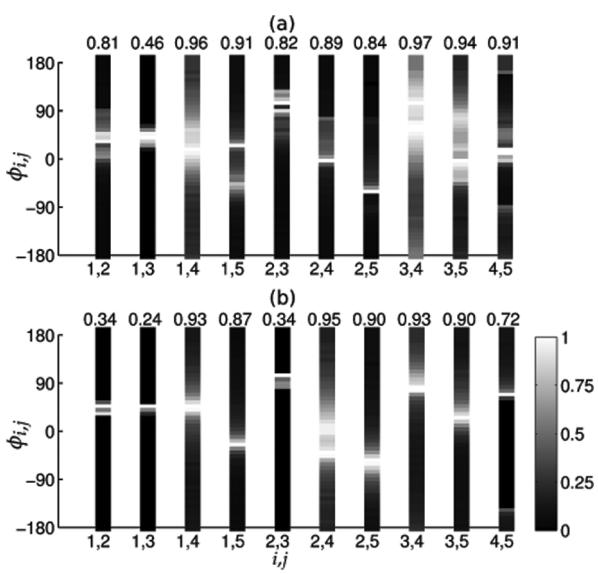


**Figure 4.** Density distribution $\phi_{i,j}$ for all pairs of oscillators (x-axis) during $SM_{T_1}$ (a) and $SM_{T_2}$ (b). The y-axis shows the phase relation from $-180$ to 180 degrees. The gray scale (see color bar) represents the density of a particular phase relation (y-axis) between a pair of oscillators (x-axis). Data are normalized so that the densest phase for each $\phi_{i,j}$ is equal to 1. The space from $-180$ to 180 is divided into 50 equally spaced bins. The numbers at the top of the images represent the Shannon entropy of each distribution of phase relations normalized to 1 (see equation (10)).

synchronized during $T_{1a}$, $T_{1c}$ and $T_{2a}$ with a phase difference in between $[-48, -33]$, $[33, 40]$, $[-26, 11]$ degrees, respectively.

Notice that the density distributions are the same as those of the complete phase relations $P(\phi_{1,5})$ shown in Figure 4(b) and (d). This is important for the measure of mutual information as the shuffled data maintains the entropy of the time series and increases its joint entropy in relation to others. This guarantees that any variation in the mutual information between components of $SM$ and $S_b$ e.g. $I(SM(s_1), S_b(\phi_{2,3}))$, is caused by changes in their statistical correlations measured by the joint entropy (see equation (11)).

*5.1.4 Synchronization dynamics ($S_a$).* The synchronization dynamics $S_a(t) = \langle x_{1,2}(t), \ldots, x_{4,5}(t) \rangle$ underlying $SM_{T_1}$ and $SM_{T_2}$ are shown in Figures 6(a) and 7(a). In $T_{1a}$, all five oscillators form a single synchronized cluster. At the end of $T_{1a}$, $\theta_4$ and $\theta_5$ start decreasing their real frequencies towards their natural ones ($w_4 = 10.9$ Hz, and $w_5 = 10.6$ Hz, not shown in the figure). In $T_{1b}$, $\theta_4$ and $\theta_5$ no longer participate in the synchronized cluster, which now consists of $\theta_1$, $\theta_2$ and $\theta_3$. At the end of $T_{1b}$, the frequency of $\theta_5$ is increasing and, at the beginning of $T_{1c}$, $\theta_5$ joins the synchronized cluster, which now consists of $\theta_1$, $\theta_2$, $\theta_3$ and $\theta_5$. The frequency of $\theta_4$ starts increasing at the beginning of $T_{1c}$ and during the
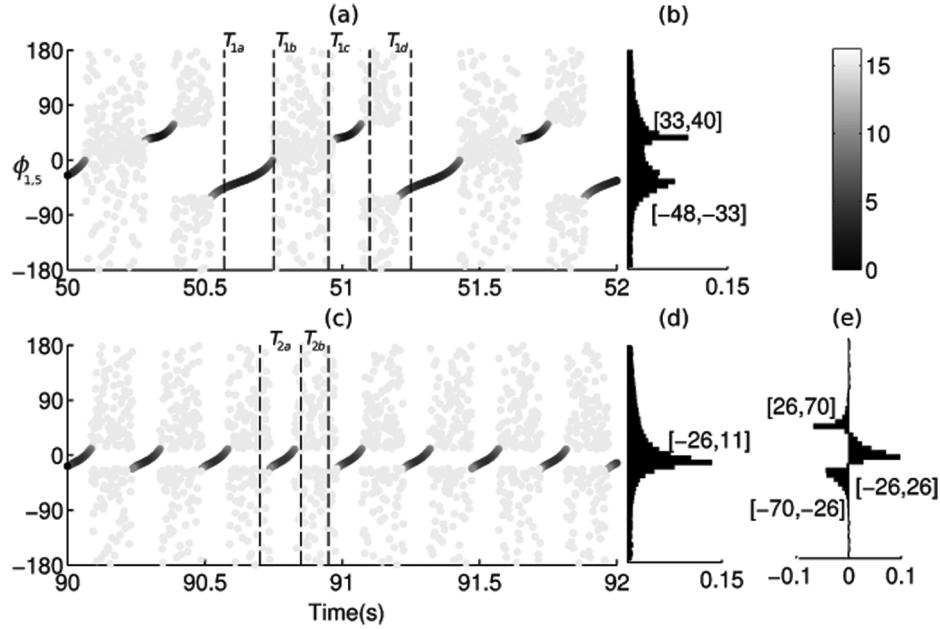
**Figure 5.** Synchronization dynamics for $\theta_1$ and $\theta_5$ ($S_b(\phi_{1,5})$) underlying sensorimotor regimes $SM_{T_1}$ (a) and $SM_{T_2}$ (c). The relation $\phi_{1,5}$ is shown in the y-axis and time in the x-axis. The color bar shows $\dot{\phi}_{1,5}$, where the darker the color the lower the derivative. Dashed lines highlight the small time-windows $T_{1a}$, $T_{1b}$, $T_{1c}$ and $T_{1d}$ (a) and $T_{2a}$ and $T_{2b}$ (c). These images were generated for $t_s = 15$ rad/s. The disperse gray dots represent phase relations that were shuffled. The derivative $\dot{\phi}_{1,5}$ is greater than 15 rad/s during the entire time-windows $T_{1b}$ and $T_{2b}$. (b) and (d) show the density distribution of each regime of phase relation. (e) shows the difference on the density distributions.
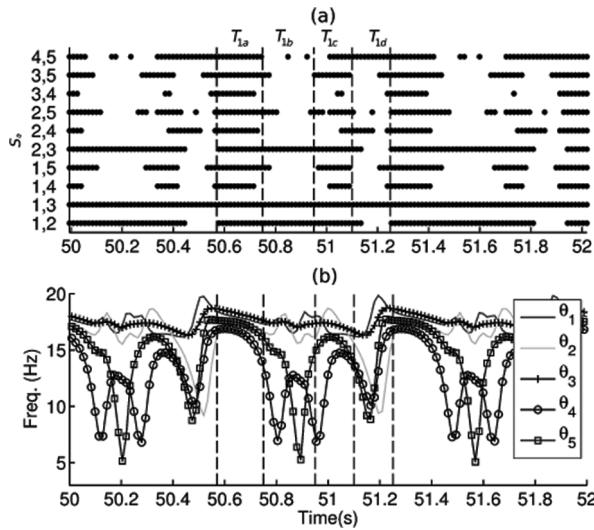


**Figure 6.** (a) shows the synchronization dynamics for the multivariate time series $S_a$ underlying $SM_{T_1}$. The y-axis contains all pairs of oscillators and each black point in the image corresponds to a moment of synchrony. (b) shows the frequency dynamics of all five oscillators (see legend).

second half of this time-window it is $\approx 15$ Hz, which is near the frequency of the others oscillators. In $T_{1d}$ two synchronized clusters emerge; the first one consisting of $\theta_1$ and $\theta_3$ at [16, 20] Hz and the second one consisting of $\theta_4$ and $\theta_5$ (see their frequency regimes in (b)). The

oscillator $\theta_2$ also joins the second synchronized cluster delayed by a small time lag (see the real frequency of $\theta_2$ in (b)). In this time-window $\theta_2$ leaves the area near its natural frequency ($w_2 = [14.5, 15.2]$ Hz, not shown in the image) and joins the second cluster at a lower frequency ($\approx 10$ Hz). At the end of $T_{1d}$, all oscillators synchronize again and a similar regime of transiently synchronized clusters as in $T_{1a}$, $T_{1b}$, $T_{1c}$ and $T_{1d}$ repeats over and over until the end of $T_1$.

The synchronization dynamics underlying $SM_{T_2}$ are simpler than those underlying $SM_{T_1}$ (see Figure 7). In $T_{2a}$, all five oscillators form a single synchronized cluster with $\theta_4$, $\theta_5$ joining the assembly slightly delayed. In $T_{2b}$, $\theta_4$ and $\theta_5$ fall apart leaving the synchronized cluster with $\theta_1$, $\theta_2$ and $\theta_3$. A similar regime of synchronization (as in $T_{2a}$, $T_{2b}$) repeats over and over until the end of $T_2$.

In this section we have analyzed the dynamics of the embodied oscillatory network underlying short intervals of the agent's sensorimotor coordination. Three dynamical descriptions of the oscillatory dynamics have been presented: $P$, $S_a$ and $S_b$. The phase relation dynamics $P$ provided a complete description of the oscillations, we have studied particularly $P(\phi_{1,5})$. The synchronization dynamics $S_b$ provided the dynamics during moments of synchrony and left out the information about the phase relations during moments of desynchronization. The binary synchronization dynamics $S_a$ provided only the information whether a
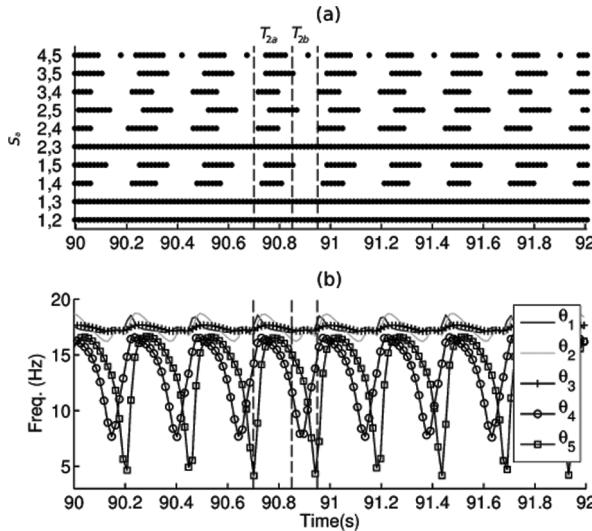
**Figure 7.** (a) shows the synchronization dynamics $S_a$ underlying $SM_{T_2}$. Each black point corresponds to a moment of synchrony between the pair of oscillators depicted in the y-axis. (b) shows the frequency dynamics of all five oscillators (see legend).



**Figure 8.** (a) shows the entropy (y-axis) of each sensorimotor component (see legend) during the agent's lifetime (x-axis). Straight dotted line at the top ($y = 5.64$ bits) represents the maximum possible value for the entropies. (b) shows the mutual information between four combinations of components from $SM$ and $P$, namely $I(SM(s_1); P(\phi_{5,4}))$, $I(SM(s_2); P(\phi_{5,1}))$, $I(SM(m_1); P(\phi_{4,3}))$ and $I(SM(m_2); P(\phi_{3,2}))$, see legend.

pair of oscillators was either synchronized or not and left out the phase of synchrony. In the next section we analyze how the information present in $S_b$ about the $SM$ varies as the value of $t_s$ decreases. In other words, we analyze whether and how the information present in oscillatory dynamics changes as reduced descriptions of phase relations are considered.

### 5.2 Informational content in reduced descriptions of P

Figure 8(a) presents the individual entropies of the sensorimotor components $s_1$, $s_2$, $m_1$ and $m_2$. During the whole trial, the entropies maintain around 5 and 5.5 bits with higher variations from 80 s, which corresponds to the moment where the agent starts moving around the light. The mean entropies for each component over the whole trial are $\overline{H(s_1)} = 5.34$, $\overline{H(s_2)} = 5.38$, $\overline{H(m_1)} = 5.03$ and $\overline{H(m_2)} = 5.21$ bits (values not shown in the image).

The mutual information between a component from $SM$ and another from the complete description $P$ are presented in Figure 8(b). Though the sensor $s_1$ has a mean entropy $\overline{H(s_1)} = 5.34$ bits, the highest mutual information between $s_1$ and the network phase relations is given by $I(SM(s_1); P(\phi_{5,4}))$ which has a peak of 1.74 bits at the beginning of the agent's lifetime – see dark black line in Figure 8(b) – and a mean $\overline{I(SM(s_1); P(\phi_{5,4}))} = 1.17$ bits over the trial. The highest mutual information between $s_2$ and the phase relations is given by $I(SM(s_2); P(\phi_{5,1}))$ with a peak of 2.05 bits at 90 s – see gray line in Figure 8(b) – and a mean

$\overline{I(SM(s_2); P(\phi_{5,1}))} = 2.05$ bits over the trial. The high values of $H(s_1)$ and $H(s_2)$ (around 5 bits) and the low values $I(SM(s_1); P(\phi_{i,j}))$ and $I(SM(s_2); P(\phi_{i,j}))$ suggest that the information about the sensory dynamics is distributed over the network.

The mutual information between motors and phase relations is high in the relation $\phi_{4,3}$, as shown by $I(SM(m_1); P(\phi_{4,3}))$ in Figure 8(b). This high value is expected as $m_1$ is controlled by $\phi_{4,3}$, as in equation (5). The value of $I(SM(m_2); P(\phi_{5,3}))$ (not shown in the figure) is also high as $m_2$ is controlled by the relation $\phi_{5,3}$. Despite the predominance of information about $m_1$ and $m_2$ in $\phi_{4,3}$ and $\phi_{5,3}$, respectively; the other phase relations also contain information about the motor dynamics. $I(SM(m_2); P(\phi_{3,2}))$, for instance, maintains near 2.5 bits during the first ~75 s and then it decays to $[0.5, 1.5]$ bits with a peak around 145 s, see dashed line in Figure 8(b).

We have shown the mutual information between four different pairs of components, but in total there are 40 possible combinations considering 4 elements in $SM$ and 10 in $P$ (or $S_b$). In order to capture how the mutual information in the phase relations decreases as $P$ is reduced to $S_b$ we take the mean of all 40 possible combinations of mutual informations, which will be referred to as $I(SM, P)$ and $I(SM, S_b)$ for the complete and reduced dynamical descriptions, respectively. Figure 9
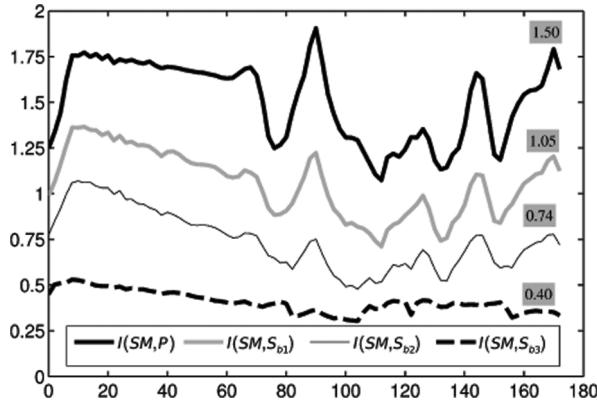
**Figure 9.** Mean mutual information between all 40 pairs of sensorimotor and phase relation components. $I(SM,P)$ shows the maximum mutual information in the phase relations throughout the trial (see time in the x-axis). $I(SM,S_{b1})$, $I(SM,S_{b2})$ and $I(SM,S_{b3})$ represent the mutual information from three reduced description with thresholds $t_s = 18$, $t_s = 9$ and $t_s = 3$ rad/s respectively. The lower the $t_s$ the less information present in the reduced descriptions. The numbers highlighted with gray background at the end of each line represent the mean mutual information over the whole trial, namely $\overline{I(SM,P)} = 1.50$, $\overline{I(SM,S_{b1})} = 1.05$, $\overline{I(SM,S_{b2})} = 0.74$, and $\overline{I(SM,S_{b3})} = 0.40$ bits.

presents $I(SM, P)$ and $I(SM, S_b)$ for three different values of $t_s$. The highest mean mutual information over the trial is given by the complete description $\overline{I(SM,P)} = 1.50$ bits. As $P$ is reduced by decreasing the threshold $t_s$ the mutual information also decreases. For the values of $t_s$ analyzed $t_s = 18$, $t_s = 9$ and $t_s = 3$, the mutual information reduced to $\overline{I(SM, S_{b1})} = 1.05$, $\overline{I(SM, S_{b2})} = 0.74$, and $\overline{I(SM, S_{b3})} = 0.40$ bits, respectively.

In order to analyze the relation between mutual information and different values of threshold, the mean $\overline{I(SM, S_b)}$ is used. The maximum value of $\overline{I(SM, S_b)}$ is 1.50 bits which is obtained with a high value of $t_s$ that makes $S_b = P$; in our model, $S_b = P$ when $t_s = 90$. In order to get a better visualization of the decay in mutual information as the value of $t_s$ decreases, the maximum mutual information $\overline{I(SM, S_b)} = 1.50$ bits for $t_s = 90$ was rescaled to 1 (see Figure 10(a)).

As the threshold decreases from 90 to 40, the phase relation loses only 10% of its information about the sensorimotor dynamics, as shown by $\overline{I(SM, S_b)} = 1$ for $t_s = 90$, and $\overline{I(SM, S_b)} = 0.9$ for $t_s = 40$ rad/s. As $t_s$ decreases the rate of decay for $\overline{I(SM, S_b)}$ increases. For $t_s = 20$ rad/s the phase relations still carry 0.73 of the total information and from $t_s = 20$ to $t_s = 1$ the information drops to 0.21. The rapid decay of information for low values of $t_s$ initially suggests that the more synchronized the phase relations the more information they carry about sensorimotor dynamics.

This result, however, should be analyzed together with the quantity of (de)synchronized phase relations
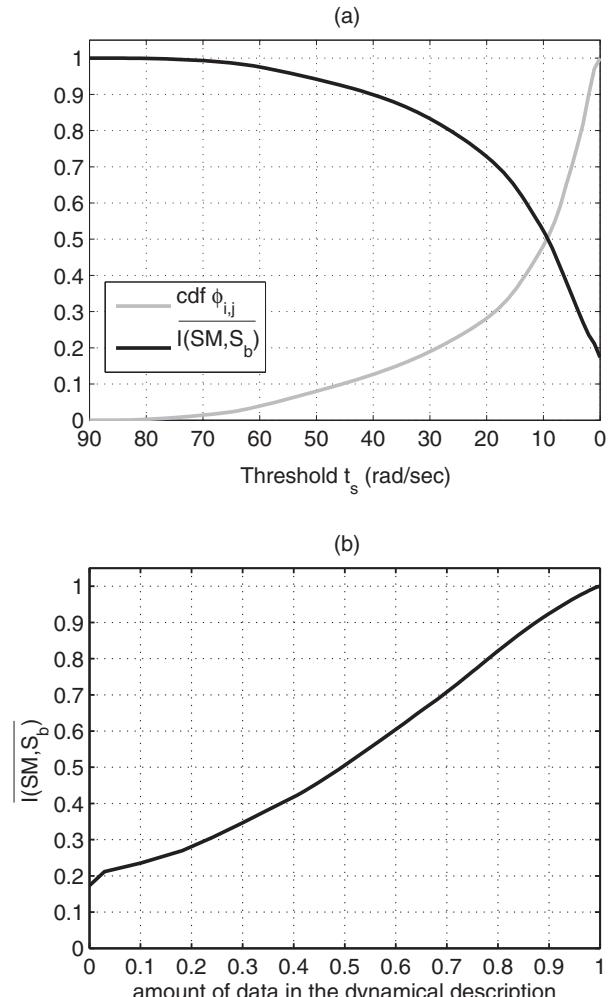




**Figure 10.** Mutual information between the phase relations and the sensorimotor dynamics for different values of $t_s$. The black line in (a) shows how $\overline{I(SM,S_b)}$ changes as the threshold $t_s$ decreases (notice inverted x-axis). The values of $\overline{I(SM,S_b)}$ are normalized in [0,1] with 1 representing the maximum $\overline{I(SM,S_b)} = 1.50$ bits. The gray line shows the cumulative function distribution (cdf) of $\dot{\phi}_{i,j}$. It represents the quantity of $\dot{\phi}_{i,j}$ greater than a $t_s$; for instance, 20% of $\dot{\phi}_{i,j}$ are greater than 30 rad/s. (b) shows how $\overline{I(SM,S_b)}$ (y-axis) changes in relation to the amount of data in the dynamical descriptions (i.e. the quantity of phase relations considered to be synchronized), where the maximum value $I$ (x-axis) represents the complete description and smaller values represent reduced descriptions obtained by decreasing the threshold. For instance, when $S_b$ contains 0.3 of the dynamics of phase relations (the other 0.7 are desynchronized oscillations) then $\overline{I(SM,S_b)} = 0.34$; i.e. 30% of the most synchronized oscillations carry 34% of the total amount of information about sensorimotor dynamics; the other 70% of oscillations, which are desynchronized, carry the remaining 66% of the total information.

for each threshold. If the values of $\dot{\phi}_{i,j}$ were uniformly distributed in the range [0,90], then just by moving the threshold we would know the quantity of synchronized and desynchronized phase relations. As in our model,

this distribution is not uniform, represented by the gray line in Figure 10(a), it is important to analyze how the mutual information $\overline{I(SM, S_b)}$ changes in relation to the amount of data in the reduced description (i.e. the quantity of phase relations considered to be synchronized), as presented in Figure 10(b). As the amount of data in the dynamical description increases – by increasing the threshold – the mutual information $\overline{I(SM, S_b)}$ also increases at a linear rate. When half of the most synchronized oscillations are included in the dynamical description then $\overline{I(SM, S_b)} = 0.51$, meaning that half of the phase relation dynamics carry half of the information about the sensorimotor dynamics.

The linear relation between the mutual information and the amount of data in the dynamical description suggests that *neither synchronized nor desynchronized oscillations carry a privileged status in terms of informational content about sensorimotor dynamics*. The informational content is equally distributed throughout the entire range of phase relations. The more a dynamical description leaves phase relations in the oscillatory network out of the equation, the less information it carries about the sensorimotor coordination, independently whether the left-out phase relations represent either synchronous or desynchronous oscillations.

### 5.3 Causal relevance of synchronous and desynchronous oscillations

In this section we present the experiment we carried out to investigate the causal relevance of desynchronous and synchronous oscillations in the generation of functional sensorimotor dynamics. In the experiment we compare the agent's behavioral performance using the fitness function in equation (8) after applying perturbations to its oscillatory network in either of the situations: during moments of synchronization ($\dot{\phi}_{i,j}(t) \leqslant t_s$), or during moments of desynchronization ($\dot{\phi}_{i,j}(t) > t_s$). The perturbation is applied to the connections between the oscillators $i$ and $j$ ($k_{i,j}$ and $k_{j,i}$) by adding a random number from a Gaussian distribution ($\mu = 0$, $\sigma^2 = \alpha k_{i,j}$), where $\alpha$ is a perturbation level parameter. If the agent's performance equally drops under the same perturbation level $\alpha$ applied to synchronous and desynchronous oscillations then it indicates that both oscillatory dynamics have the same relevance to the generation of functional sensorimotor coordinations. On the other hand, if the performance does not decay equally then the oscillatory dynamics that cause a greater decay are the more relevant.

A critical point of this experiment is the *threshold* from which an oscillation is considered to be either synchronized or desynchronized. If we consider, for instance, that synchronous oscillations are below 2 rad/s then perturbations applied to desynchronous oscillations will probably cause a greater decay in the
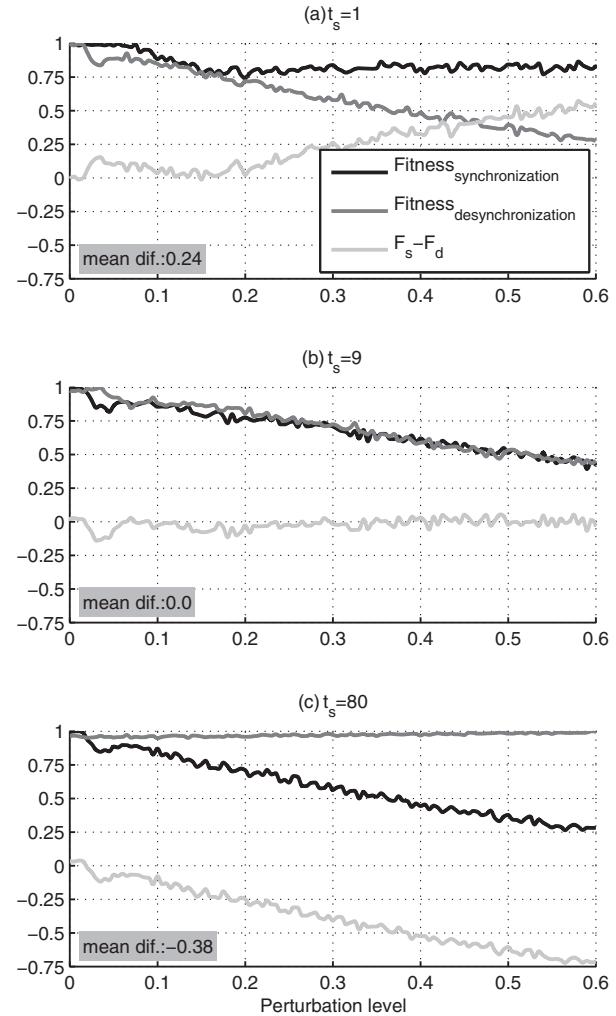


**Figure 11.** Agent's fitness (y-axis) for different levels of perturbations $\alpha$ (x-axis) and thresholds $t_s = 1$ (a), $t_s = 9$ (b), and $t_s = 80$ (c). Black and dark-gray lines show the fitnesses of the agent when perturbation is applied to synchronous and desynchronous oscillations, respectively (see legend). The light-gray line is the fitness difference $Fitness_{synchronization} - Fitness_{desynchronization}$ (see legend). The numbers highlighted with a gray background show the mean of the fitness difference over all perturbation levels. This mean will be referred to as $\overline{F_s - F_d}$.

agent's performance as the range of perturbations is wider ($\dot{\phi}_{i,j} > 2$ rad/s). Figure 11 presents the agent's fitness for three different values of thresholds $t_s$ and perturbation levels $\alpha$. Each fitness represents an average over 200 trials.

For $t_s = 1$, desynchronized oscillations are more relevant than synchronized ones to the agent's performance, which can be seen by the fitness difference (gray line) and by $\overline{F_s - F_d} = 0.24$. Notice that for $t_s = 1$ and $\alpha < 0.1$ (see (a)) the agent's performance is not affected when perturbations are applied to synchronous oscillations. As $\alpha$ increases from 0.1 to 0.2 both fitnesses decay, and for $\alpha > 2$ the perturbations to desynchronous oscillations have a greater effect on the agent's fitness,
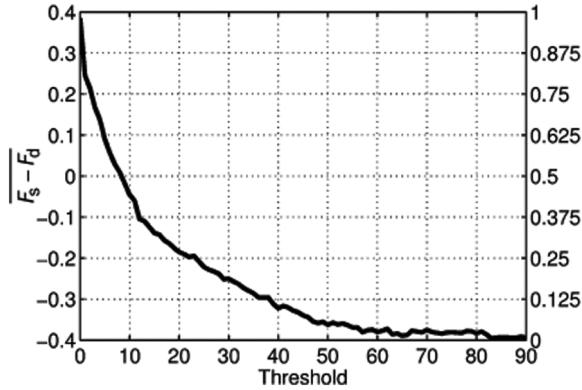
**Figure 12.** Mean of fitness difference $\overline{F_s - F_d}$ (y-axis on the left) for different thresholds $t_s$ (x-axis). Positive values indicate that desynchronization is more relevant than synchronization for the generation of functional sensorimotor coordination. The y-axis on the right side represents $\overline{F_s - F_d}$ rescaled to [0,1]. When the rescaled $\overline{F_s - F_d}$ is 0.5, for instance, both types of oscillations are equally relevant. The rescaled $\overline{F_s - F_d}$ works as an index of relevance for desynchronous oscillations, where 0 indicates no relevance and 1 maximum relevance.

as shown by an increase in the fitness difference. For $t_s = 9$, both types of oscillations are equally important as the fitness difference maintains near zero for all levels of perturbation which gives a mean $\overline{F_s - F_d} = 0$. For $t_s = 80$, all levels of perturbation to desynchronous oscillations do not affect the agent's performance (dark-gray line maintains near 1 for all perturbations). The reason for that is that there are very few occurrences ($\approx 0.04\%$) of $\dot{\phi}_{i,j} > 80$ rad/s.

In order to analyze how the relevance of desynchronous oscillations changes in relation to the threshold, the mean of the fitness difference $(\overline{F_s - F_d})$ is used (see Figure 12). The values of $\overline{F_s - F_d}$ vary within $\approx [-0.4, 0.4]$, where $-0.4$ indicates that desynchronization is not relevant for sensorimotor behavior and 0.4 indicates its maximum relevance. This interval is also presented in a scale $[0,1]$ – right y-axis in Figure 12 – and from now on we will use this scale to discuss the relevance of desynchronous oscillations. For values of threshold below $\approx 7$ rad/s desynchronous oscillations are more relevant than synchronous ones, which can be seen by $\overline{F_s - F_d} > 0.5$. Both types of oscillations are equally relevant when $t_s \approx [7, 11]$ and above this range the relevance of desynchronous oscillations is smaller. For $t_s = 40$, for instance, desynchronization has $\approx 0.125$ of relevance to the agent's sensorimotor coordination. The relevance of desynchronous oscillations measured only in terms of the threshold do not take into account the distribution of $\dot{\phi}_{i,j}$ over the range $[0,90]$. Similarly to the analysis of mutual information presented in the previous section, a more robust measure of causal relevance should also consider the distribution of $\dot{\phi}_{i,j}$.
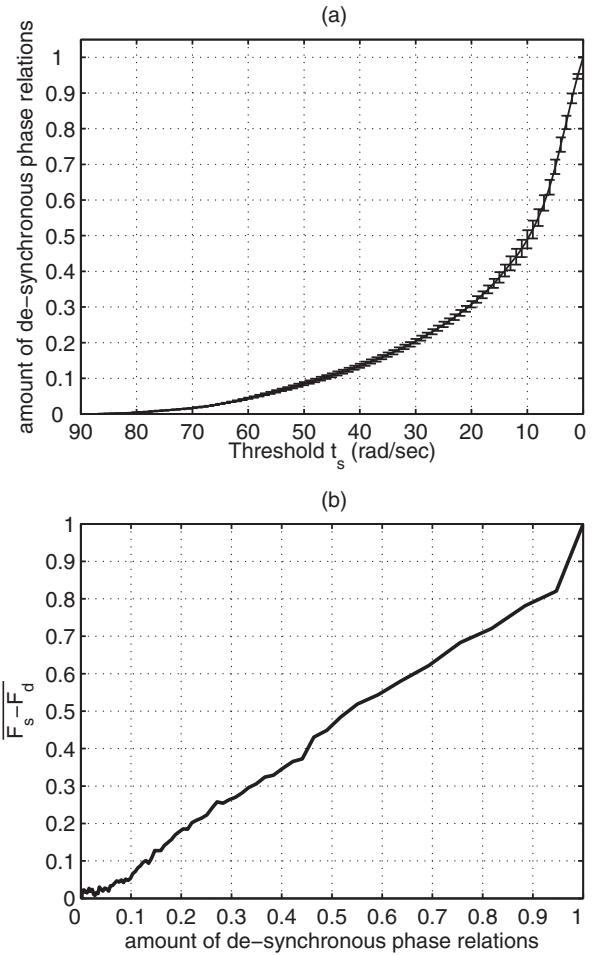


**Figure 13.** (a) shows how the quantity of desynchronous phase relations changes (y-axis) for different thresholds (x-axis). Bars represent the standard deviations. Near 50% of the phase relations have their derivative $\dot{\phi}_{i,j} < 10$ rad/s. (b) shows how the relevance of desynchronized oscillations, i.e. $\overline{F_s - F_d}$ rescaled to [0,1], changes in relation to the quantity of phase relations considered desynchronized (x-axis).

As the threshold increases, the quantity of phase relations that are considered desynchronized decreases, this relation is represented by the distribution function of $\dot{\phi}_{i,j}$ shown in Figure 13(a). This result is similar to the one presented for the single agent we analyzed in the previous section; here, however, we perturbed the desynchronous oscillations with $\alpha \in [0, 0.6]$ and for each pair $(\alpha, t_s)$ we ran 200 trails. When $t_s = 20$, 0.30 of the total number of phase relations are desynchronized, and when $t_s$ increases to $t_s = 40$, for instance, the number of desynchronized phase relations decreases to 0.13 of the total phase relations.

Figure 13(b) shows the relevance of desynchronized oscillations, i.e. $\overline{F_s - F_d}$, in relation to the quantity of phase relations considered desynchronized, i.e. $\dot{\phi}_{i,j} > t_s$. When 0.5 of the total number of phase relations – which includes all $\dot{\phi}_{i,j} > 10$ – are considered

desynchronized then these oscillations will have 0.48 of relevance for the agent's fitness; and when 0.95 of the total number of phase relations – which includes all $\dot{\phi}_{i,j} > 1$ – are considered desynchronized then these oscillations will have 0.82 of relevance. Notice that the synchronized phase relations below 1 rad/s actually play an important role in the generation of the agent's behavior. While 0.95 of phase relations – which includes all $\dot{\phi}_{i,j} > 1$ – has 0.82 of relevance, the remaining 0.05 of phase relations – which includes all $\dot{\phi}_{i,j} \leqslant 1$ – has 0.18 of relevance.

This result indicates that oscillations synchronized with a narrow window of frequency difference – in our model this window was of 1 rad/s in a range of frequency differences from 0 to 90 rad/s – are relatively more causally relevant for the generation of functional sensorimotor coordination than the rest of the oscillations with higher frequency differences. That is not to say that the 'rest' of the oscillations are not relevant, as they still carry 0.82 of relevance. Apart from the range of $\dot{\phi}_{i,j} \leqslant 1$, the causal relevance of the phase relations is distributed over the range of possible $\dot{\phi}_{i,j}$ values without any privileged status of causal relevance to either synchronous or desynchronous oscillations

## 6  Discussion and conclusion

As far as methodological aspects are concerned, we have combined evolutionary robotics with Kuramoto oscillators to study the roles played by synchronous and desynchronous oscillations in the context of a sensorimotor coordination task. We have used information–theoretic measures and dynamical system concepts to analyze the system. The model was not meant to target any specific level of abstraction from individual neurons and very small circuits (Izhikevich, 2007) to the whole cortex and brain activity (Buzsaki, 2006; Varela et al., 2001). Our goal was rather to reproduce at a merely conceptual level of generality the *type* of data from which the significance of synchronization is generally privileged and to show how a system does in fact functionally exploit the whole phase dynamic to achieve a coherent sensorimotor coordination. Such a proof of concept should not be taken as an empirical model – see Barandiaran and Moreno (2006), for a distinction between conceptual and empirical models.

The results obtained from the analysis of the model give some insights to help answer the question: *how does the informational content of the sensorimotor activity present in a complete dynamical description of phase relations change as such a description is reduced to the dynamics of synchronous oscillations?* In our particular model, the informational content was equally distributed throughout the entire range of phase relations; the more the dynamical description was reduced the less information it carried about the sensorimotor

coordination. Neither synchronized nor desynchronized oscillations was found to carry a privileged status in terms of informational content in relation to the agent's sensorimotor activity. It is important to notice that the analysis we have presented not only suggests that the phase relations of desynchronous oscillations carry relevant information about sensorimotor behavior but, more importantly, it shows *how* the informational content changes as the dynamical description of the oscillatory network is reduced by gradually removing the phase relation dynamics of desynchronous oscillations.

The results also gave some insights to address the questions: *to what extent are desynchronous oscillations as causally relevant as synchronous ones to the generation of functional sensorimotor coordination?* In our particular model, although the phase relations of oscillations with a narrow frequency difference carried a relatively higher causal relevance than the rest of the phase relations to sensorimotor coordinations, overall there was no privileged functional causal contribution to either synchronous or desynchronous oscillations. Notice that the analysis we have presented not only suggests that desynchronized neural activity has functional significance to sensorimotor behavior but, more importantly, it shows the relevance of desynchronous oscillations in relation to synchronous ones considering a gradual reduction of the threshold delimiting both types of oscillations.

Some contemporary cognitive neuroscience studies focus on synchronized activities between different brain areas after a given stimuli onset and assume that such activities are functional units representing the stimuli. The high level of synchronization found by empirical experiments represents only part of the explanatory picture that involves all of the phase relations and, as our results have suggested, the reduction of phase relations to synchrony might be hindering relevant information about neural oscillatory activity. Thus, an alternative procedure would consider the entire regime of phase relations between distinct brain areas as the functional unit (causally) correlated to the stimuli.

## References

Barandiaran, X. & Moreno, A. (2006). ALife models as epistemic artefacts. In: *10th international conference on artificial life*, pp. 513–519. Cambridge, MA: MIT Press.

Beer, R. D. (2003). The dynamics of active categorical perception in an evolved model agent. *Adaptive Behavior, 11*, 209–243.

Breakspear, M., Heitmann, S., & Daffertshofer, A. (2010). Generative models of cortical oscillations: neurobiological implications of the kuramoto model. *Frontiers in Human Neuroscience, 4*, 190.

Bressler, S. L., Coppola, R., & Nakamura, R. (1993). Episodic multiregional cortical coherence at multiple frequencies during visual task performance. *Nature, 366*, 153–156.

Buzsaki, G. (2006). *Rhythms of the brain*. Oxford, UK: Oxford University Press.

Ceguerra, R. V., Lizier, J. T., & Zomaya, A. Y. (2011). Information storage and transfer in the synchronization process in locally-connected networks. In: *IEEE symposium series in computational intelligence*, pp. 54–61. Piscataway, NJ: IEEE Press.

Cover, T. M. & Thomas, J. A. (2005). *Elements of information theory*. Hoboken, NJ: John Wiley & Sons.

Dano, S., Sorensen, P. G., & Hynne, F. (1999). Sustained oscillations in living cells. *Nature, 402*, 320–322.

Eckhorn, R., Bauer, R., Jordan, W., Brosch, M., Kruse, W., Munk, M., and Reitboeck, H. J. (1988). Coherent oscillations: a mechanism of feature linking in the visual cortex? *Biological Cybernetics, 60*, 121–130.

Engel, A. K., Konig, P., Gray, C. M., & Singer, W. (1990). Stimulus-dependent neuronal oscillations in cat visual cortex: inter-columnar interaction as determined by cross-correlation analysis. *European Journal of Neuroscience, 2*, 588–606.

Engel, A., Konig, P., Kreiter, A., & Singer, W. (1991). Interhemispheric synchronization of oscillatory neuronal responses in cat visual cortex. *Science, 252*, 1177–1179.

Fries, P. (2005). A mechanism for cognitive dynamics: neuronal communication through neuronal coherence. *Trends in Cognitive Sciences, 9*, 474–480.

Gardner, M., Hubbard, K., Hotta, C., Dodd, A., & Webb, A. (2006). How plants tell the time. *Biochemical Journal, 397*, 15–24.

Gray, C. M. & Singer, W. (1989). Stimulus-specific neuronal oscillations in orientation columns of cat visual cortex. *Proceedings of the National Academy of Sciences of the United States of America, 86*, 1698–1702.

Harvey, I. (2001). Artificial evolution: a continuing SAGA. In: *8th international symposium on evolutionary robotics*. Berlin: Springer-Verlag.

Harvey, I., Husbands, P., Cliff, D., Thompson, A., & Jakobi, N. (1997). Evolutionary robotics: the sussex approach. *Robotics and Autonomous Systems, 20*, 205–224.

Harvey, I., Paolo, E. D., Wood, R., & Quinn, M. (2005). Evolutionary robotics: a new scientific tool for studying cognition. *Artificial Life, 11*, 79–98.

Hipp, J. F., Engel, A. K., & Siegel, M. (2011). Oscillatory synchronization in large-scale cortical networks predicts perception. *Neuron, 69*, 387–396.

Huygens, C. (1673). *Horologium oscillatorium sive de motu pendulorum ad horologia aptato demonstrationes geometricae*. Paris, France: F. Muguet.

Izhikevich, E. M. (2007). *Dynamical systems in neuroscience: the geometry of excitability and bursting*. Cambridge, MA: MIT Press.

Izquierdo, E. J. & Lockery, S. R. (2010). Evolution and analysis of minimal neural circuits for klinotaxis in caenorhabditis elegans. *Journal of Neuroscience, 30*, 12908–12917.

Kitzbichler, M. G., Smith, M. L., Christensen, S. R., & Bullmore, E. (2009). Broadband criticality of human brain network synchronization. *PLoS Computational Biology, 5*, e1000314.

Kozyreff, G., Vladimirov, A. G., & Mandel, P. (2000). Global coupling with time delay in an array of semiconductor lasers. *Physical Review Letters, 85*, 3809–3812.

Kuramoto, Y. (1984). *Chemical oscillations, waves, and turbulence*. New York, NY: Springer.

Lungarella, M. & Sporns, O. (2006). Mapping information flow in sensorimotor networks. *PLoS Computational Biology, 2*, e144.

Lutz, A., Lachaux, J., Martinerie, J., & Varela, F. J. (2002). Guiding the study of brain dynamics by using firstperson data: Synchrony patterns correlate with ongoing conscious states during a simple visual task. *Proceedings of the National Academy of Sciences of the United States of America, 99*, 1586–1591.

Moioli, R. C., Vargas, P. A., & Husbands, P. (2010). Exploring the kuramoto model of coupled oscillators in minimally cognitive evolutionary robotics tasks. In: *IEEE world congress on computational intelligence*, pp. 1–8. Piscataway, NJ: IEEE Press.

Nolfi, S. & Floreano, D. (2004). *Evolutionary robotics: the biology, intelligence, and technology of self-organizing machines*. Scituate, MA: Bradford Company.

Pikovsky, A., Rosenblum, M., & Kurths, J. (2003). *Synchronization: a universal concept in nonlinear sciences*. Cambridge, UK: Cambridge University Press.

Pitti, A., Lungarella, M., & Kuniyoshi, Y. (2009). Generating spatiotemporal joint torque patterns from dynamical synchronization of distributed pattern generators. *Front Neurorobotics, 3*, 2.

Pockett, S., Bold, G. E., & Freeman, W. J. (2009). EEG synchrony during a perceptual-cognitive task: Widespread phase synchrony at all frequencies. *Clinical Neurophysiology, 120*, 695–708.

Rodriguez, E., George, N., Lachaux, J., Martinerie, J., Renault, B., and Varela, F. (1999). Perception's shadow: long-distance synchronization of human brain activity. *Nature, 397*, 430–433.

Roelfsema, P. R., Engel, A. K., Konig, P., & Singer, W. (1997). Visuomotor integration is associated with zero time-lag synchronization among cortical areas. *Nature, 385*, 157–161.

Roskies, A. L. (1999). The binding problem. *Neuron, 24*, 7–9.

Ruppin, E. (2002). Evolutionary autonomous agents: a neuroscience perspective. *Nature Reviews Neuroscience, 3*, 132–141.

Santos, B. A., Barandiaran, X. E., & Husbands, P. (2011). Metastable dynamical regimes in an oscillatory network modulated by an agent's sensorimotor loop. In: *IEEE symposium on artificial life*, pp. 124–131. Piscataway, NJ: IEEE Press.

Shannon, C. E. (1948a). A mathematical theory of communication. *The Bell System Technical Journal, 27*, 379–423.

Shannon, C. E. (1948b). A mathematical theory of communication. *The Bell System Technical Journal, 27*, 623–656.

Singer, W. (2011). Dynamic formation of functional networks by synchronization. *Neuron, 69*, 191–193.

Strogatz, S. H. (2000a). From kuramoto to crawford: exploring the onset of synchronization in populations of coupled oscillators. *Physica D: Nonlinear Phenomena, 143*, 1–20.

Strogatz, S. H. (2000b). *Nonlinear dynamics and chaos: with applications to physics, biology, chemistry and engineering*. Jackson, TN: Perseus Books.

Tononi, G. & Edelman, G. M. (1998). Consciousness and complexity. *Science, 282*, 1846–1851.

Uhlhaas, P. J., Pipa, G., Lima, B., Melloni, L., Neuenschwander, S., Nikolic, D., & Singer, W. (2009). Neural synchrony in cortical networks: history, concept and current status. *Frontiers in Integrative Neuroscience, 3*, 17.

Varela, F., Lachaux, J., Rodriguez, E., & Martinerie, J. (2001). The brain web: phase synchronization and large-scale integration. *Nature Reviews Neuroscience, 2*, 229–239.

von der Malsburg, C. (1981). The correlation theory of brain function. Technical report, Max Planck Institute for Biophysical Chemistry.

Walker, T. J. (1969). Acoustic synchrony: two mechanisms in the snowy tree cricket. *Science, 166*, 891–894.

Williams, P. L. & Beer, R. D. (2010). Information dynamics of evolved agents. In S. Doncieux, B. Girard, A. Guillot, J. Hallam, J. Meyer, & J. Mouret (Ed.), *From animals to animats 11* (vol. 6226, pp. 38–49). Berlin, Germany: Springer.

Winfree, A. T. (1967). Biological rhythms and the behavior of populations of coupled oscillators. *Journal of Theoretical Biology, 16*, 15–42.

Winfree, A. T. (1980). *The geometry of biological time*, vol. 12. Berlin: Springer-Verlag.

## About the Authors

**Bruno A Santos** is a lecturer at the department of computer engineering in the Federal Centre of Technological Education, Minas Gerais, Brazil and a PhD student in cognitive science at the centre for computational neuroscience and robotics at the University of Sussex (UK). He is interested in researching the (oscillatory) neural dynamics underlying sensorimotor activity using models of artificial agents.



**Xabier E Barandiaran** graduated with a degree in philosophy from the University of Deusto (Spain), he obtained an MSc in evolutionary and adaptive systems at the University of Sussex, and received a PhD from the University of the Basque Country (Spain). After completing a post-doc at the centre for computational neuroscience and robotics at the University of Sussex and a second year at the centre de recherche en epistémologie appliqué (CNRS/Polytechnique, Paris) he currently hold a research contract at the IAS-research centre for life, mind and society (University of the Basque Country) working for the FP7 EU project 'extending sensorimotor contingencies to cognition'. His main research areas are the philosophy of artificial life and complex adaptive systems, enactive cognitive science and robotics, origins and minimal forms of agency and naturalized epistemology.
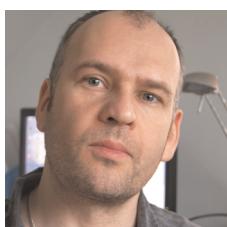


**Philip Husbands** is professor of artificial intelligence and co-director of the CCNR, University of Sussex. His research interests include biologically inspired adaptive robotics, evolutionary systems, computational neuroscience, and creative systems.